Numerical studies of mode gaps and coupling efficiency for line-defect waveguides in two-dimensional photonic crystals

M. Qiu[1,*] K. Azizi,[2] A. Karlsson,[2] M. Swillo,[2] and B. Jaskorzynska[2]
[1]*Division of Electromagnetic Theory, Royal Institute of Technology (KTH), 100 44 Stockholm, Sweden*
[2]*Laboratory of Optics, Photonics, and Quantum Electronics, Department of Microelectronics and Information Technology, Royal Institute of Technology (KTH), Electrum 229, 164 40 Kista, Sweden*
(Received 20 November 2000; revised manuscript received 20 April 2001; published 28 September 2001)

Using conventional waveguides for light coupling and collection we numerically study band structures and transmission spectra for guided modes in line-defect waveguides obtained by removing rows of air holes in a lossless triangular-lattice two-dimensional photonic crystal. The two-dimensional finite-difference time-domain method combined with the effective index method and complemented with the coupled mode approximation is employed to analyze mode-gaps (or mini stopbands) arising from Bragg diffraction of the incident mode into the counterpropagating modes. We also show that more than 97% coupling efficiency between the ridge and the photonic crystal waveguides is achievable by adjustment of the ridge waveguide width.

DOI: 10.1103/PhysRevB.64.155113 PACS number(s): 42.70.Qs, 78.20.Bh

I. INTRODUCTION

Photonic crystals (PC's) may offer a possibility of eliminating electromagnetic wave propagation within a frequency band, i.e., a photonic band gap (PBG).[1,2] In particular, ideal two-dimensional (2D) photonic crystals, which are periodic in a plane (e.g., *xy* plane) and uniform in the perpendicular direction (e.g., *z* direction), hold substantial promise for applications in optoelectronics and integrated optics due to their compactness and possibilities to engineer dispersion relations, although they do not provide full three-dimensional (3D) PBG's. For a 2D triangular lattice of air holes in a dielectric medium, the 2D PBG is larger than for their corresponding square lattice counterparts due to their more circular Brillouin zone.[2] Therefore, intensive investigations have been carried out recently on triangular photonic crystals (see, e.g., Refs. 3–12).

Although it has been demonstrated that almost ideal (holes depth much larger than the incident beam spot-size) 2D PC can be fabricated for the far-infrared wavelength range,[11,12] PC structures for the near-infrared telecommunication window are typically realized by etching holes (or rods) through a three-layer slab waveguide[3–10] which assures light confinement in the vertical direction. In the present paper we consider such structures, however, to reduce computational effort we apply the effective index approximation for the vertical direction and the 2D finite-difference time-domain (FDTD) method for the in-plane propagation, which is a good approximation assuming well confined slab modes. The out-of-plane radiation losses which may arise from inappropriate design of a slab waveguide (intrinsic loss),[13,14] or from too shallow holes[15], are not addressed in our studies.

When a line defect is introduced into a photonic crystal, the electromagnetic wave whose frequency is in the band gap can be guided along the line defect without appreciable losses. Thus, formed waveguides could be used to realize compact integrated optical circuits. PC waveguides in a photonic crystal can be obtained by removing rows of air holes (i.e., by not etching them). Thus a high index central region is achieved, in which both conventional (index confined) modes and PC modes confined by the all-reflecting photonic crystal surrounding can exist. Two geometries for the boundary between the triangular PC and the waveguide were studied in Ref. 16 (see Fig. 1 of Ref. 16): *A* type, where a waveguide is formed by an odd number of missing holes, and *B*-type waveguide with an even number of holes missing. It was found that for the *A*-type waveguide a mode splitting occurs at the edge of the Brillouin zone. The splitting can be attributed to coupling between forward and backward propagating modes of the same order arising from Bragg diffraction on the boundary holes. Similar coupling occurs in a conventional waveguide with periodically perturbed walls or in other types of waveguided distributed Bragg reflectors. Within the coupled mode theory it already was treated by Kogelnick and Shank[17]. For the *B*-type waveguides, where the boundary holes are not symmetrically located with respect to the waveguide center but *dephased* by a half of the lattice constant, the mode splitting did not occur. This is quite understandable since the coupling between the same mode, no matter what its symmetry is, cannot be caused by an antisymmetric perturbation.[18] In Ref. 19 the mode gaps, primarily at the zone edge, were discussed in more detail and their implications for localized states in waveguide bends and discontinuities were addressed. It was also briefly shown (see Fig. 4 in Ref. 19 and Figs. 2 and 3 in Ref. 12) that mode gaps, also called mini stop bands (MSB), may also occur away from the zone edge. In the present paper we study such mode gaps for the *A*-type PC waveguide in more detail and show that they occur due to contradirectional coupling between different order of modes but only of the same symmetry. This is again in analogy to coupling between phase matched, lower and higher order modes in a periodically perturbed conventional waveguide. However, because of the very high contrast of the refractive index one cannot apply the perturbation theory but a numerically exact treatment is needed. For our studies we employ the finite-difference time-domain (FDTD) method, allowing us to compute the transmission spectra of PC waveguides as a function of a number of parameters; excitation frequency, symmetry of an excita-

tion mode, or width and length of a waveguide. Moreover, in order to address the external excitation and detection problems we consider a structure consisting not only of a PC waveguide but also of two conventional, access and exit ridge waveguides, which to our knowledge has not earlier been done.

The outline of the papers is as follows. In Sec. II we show the dispersion relation for the 2D PC waveguide and introduce the mode classification. In Sec. III we give detailed numerical results of the transmission spectrum for a PC waveguide inserted between two conventional, ridge waveguides, and relate the dips in the transmission to the mini stop bands in the dispersion diagram. Mode attenuation in the mini stop band is given in terms of a coupling constant for the contradirectional coupling. We also show how the coupling efficiency depends on the relative width of the PC and the ridge waveguides. In Sec. IV we conclude the obtained results.

II. GUIDED MODES IN A PC WAVE GUIDE: DISPERSION RELATION AND MODE DENOMINATIONS

Many studies have been carried out concerning guided modes in two-dimensional dielectric photonic band gap crystals (see, e.g. Refs. 16,19–21). In the present paper, we study guided modes in a 2D dielectric photonic crystal, which is a triangular lattice of air holes in a dielectric medium corresponding to the carefully studied case of GaAs samples in Ref. 9. The effective dielectric constant of the material is $\epsilon = 11.0$, and the radius of the holes is $R = 0.32a$ (filling factor $f = 37\%$, where a is the lattice constant). It has been shown that there is a band gap for the H-polarization (TE) case,[9] between 0.22 and 0.31 (a/λ). However, there is no band gap for the E-polarization (TM) case. Thus, only H polarization is considered in the present paper. A waveguide is introduced here by removing (not etching) one or several rows of air holes in the photonic crystal. Here we denote a waveguide Wn, where n is the number of removed holes.

In this paper we will mainly present results for a W3 PC waveguide (of type A in the notation of Ref. 16). Figure 1 shows the eigenfrequencies of the guided modes in such a W3 waveguide. The eigenfrequencies of the guided modes are calculated with the 2D FDTD method, and the details of calculations can be found in Refs. 22–26. The effective index method is used to account for the vertical confinement. In the figure we have also given a mode classification (mode numbers). It can be shown that all PC waveguide modes can be related to guided modes in a conventional metallic waveguide,[19,24] in which one imposes an artificial periodicity d in the direction of the wave propagation (e.g., x direction).

The solutions for those modes in the waveguide have the following component:

$$H_z = C_0 \sin[m\pi(y/b + 1/2)] \times e^{i(2\pi n/d + k)x},$$
$$m = 1,2,3,\ldots, n = 0, \pm 1, \pm 2, \ldots, \quad (1)$$

where C_0 is a coefficient and b is the effective width of the waveguide, respectively. k is the irreducible wave vector in the Brillouin zone. A positive number (including 0) of n represents forward propagation, while a negative number of n represents backward propagation. Consequently, the modes of the conventional waveguide with the artificial periodicity can be labeled by $[m,n]$ according to the above equation (see Fig. 1). The even modes correspond to $m = 1,3,5,\ldots$ and the odd modes correspond to $m = 2,4,6,\ldots$.

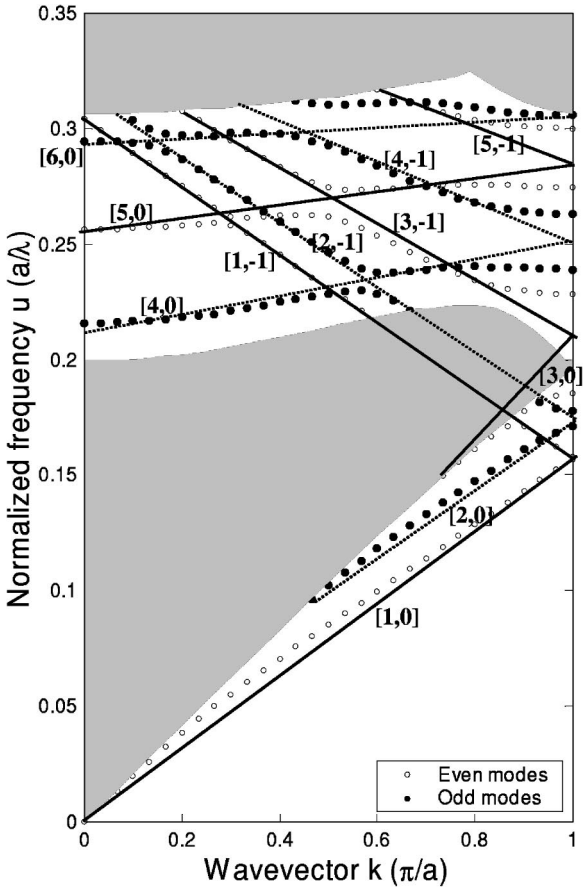

FIG. 1. The eigenfrequencies of the guided modes in the W3 waveguide obtained by removing three rows of holes. The solid lines represent the even modes, and the dotted lines represent the odd modes. The gray areas are the projected band structure of the perfect crystal.

From Fig. 1 one can see that there are two types of mode gaps. The ones occurring at the Brillouin zone edge are due to the coupling between the forward and backward propagat-

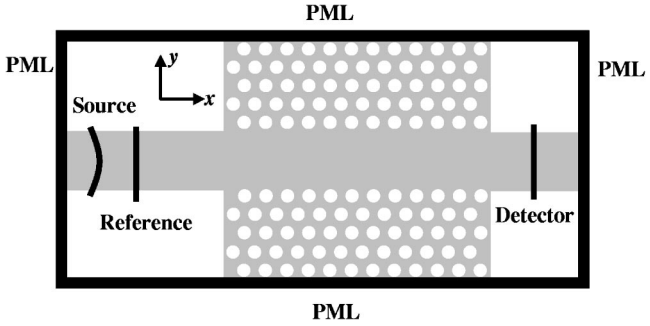

FIG. 2. Setup for the computation of the transmission through the W3 waveguide.

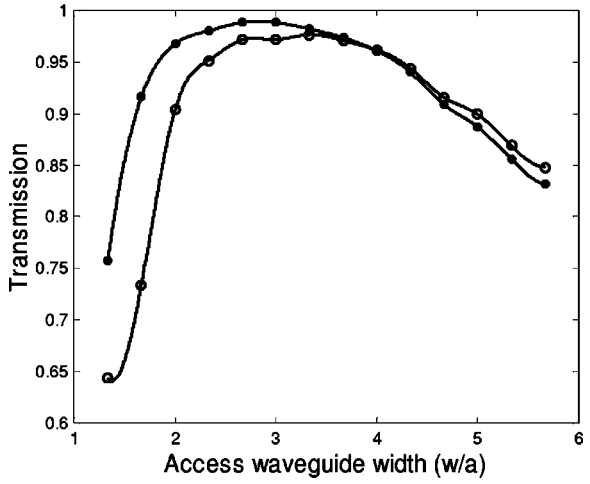

FIG. 3. The transmission from the entrance waveguide to the exit waveguide, through the W3 PC waveguide, as a function of the width of the conventional waveguide. The open circles are the average transmission for the normalized frequency range from 0.22 to 0.25 (a/λ), while the solid circles are for the normalized frequency range from 0.27 and 0.30 (a/λ).

ing modes of the same order (same value of m), i.e., the ordinary Bragg scattering of a distributed feedback (DFB) laser.[17] The other ones are mode gaps due to the contradirectional coupling between modes of different orders, e.g., the mode gap between the $[1,-1]$ mode and the $[5,0]$ mode. Since the considered W3 waveguide is of the A type, the coupling occurs only between modes of the same symmetry. Furthermore, it is worth mentioning that since the W3 waveguide has a high index central region, which supports the index confinement modes, there are guided modes below the lowest photonic crystal band.

III. ANALYSIS OF THE MODE TRANSMISSION

The 2D FDTD method combined with the effective index approximation is also used to simulate the wave propagation in the W3 waveguide. The setup for the computation is shown in Fig. 2. Since we consider a finite structure here, the whole computational domain is surrounded by perfectly matched layers[27] (PML's) to absorb the outgoing waves. In order to control the excitation conditions more accurately, a conventional dielectric waveguide is used as an entrance (and an exit) waveguide, as schematically depicted in Fig. 2. A pulse source is located at the entrance. The source is the product of the Gaussian function and the exact solution (at the center frequency) of the guided mode in the conventional waveguide. Thus, one can excite different guided modes in the W3 waveguide by introducing different solutions of the modes (i.e., different m) in the entrance waveguide. Another advantage of the current configuration is that one can easily normalize the transmission spectra, by comparing the Poynting vector at the reference line and the detector line (see Fig. 2).

Experimentally, only the fundamental guided mode ($m=1$) is usually involved due to the excitation scheme of the experimental setup.[9,10,28] Therefore, we first consider the fundamental guided mode. For this mode, the transmission from the conventional waveguide to the PC waveguide could be very high, if the width of the conventional waveguide is carefully adjusted. Figure 3 shows the transmission from the entrance waveguide to the exit waveguide, through the W3 PC waveguide, as a function of the width of the conventional waveguide. The open circles are the average transmission for the normalized frequency range from 0.22 to 0.25 (a/λ), while the solid circles are for the normalized frequency range from 0.27 and 0.30 (a/λ). When the width of the conventional waveguide is about 2.6 a, the transmissions have their maximums for both the frequency ranges (more than 97% transmission). For the W3 waveguide, the distance between the opposite air holes in the waveguide boundary is about 2.8 a. Therefore, when the conventional waveguide width is similar as the PC waveguide width, one can obtain a very high coupling efficiency. In the following calculations, the width of the entrance and the exit waveguides is fixed to 2.6 a.

Figure 4 shows the calculated transmission spectra of the fundamental mode $(m=1)$ for different lengths of the W3 waveguide. The edge of the photonic band gap is indicated by gray lines. One can easily see from the figure that there is a mini stop band (MSB) in the band gap, centered at the normalized frequency 0.26 (a/λ), which is in good agreement with the experimental result 0.263 (a/λ).[28] When the

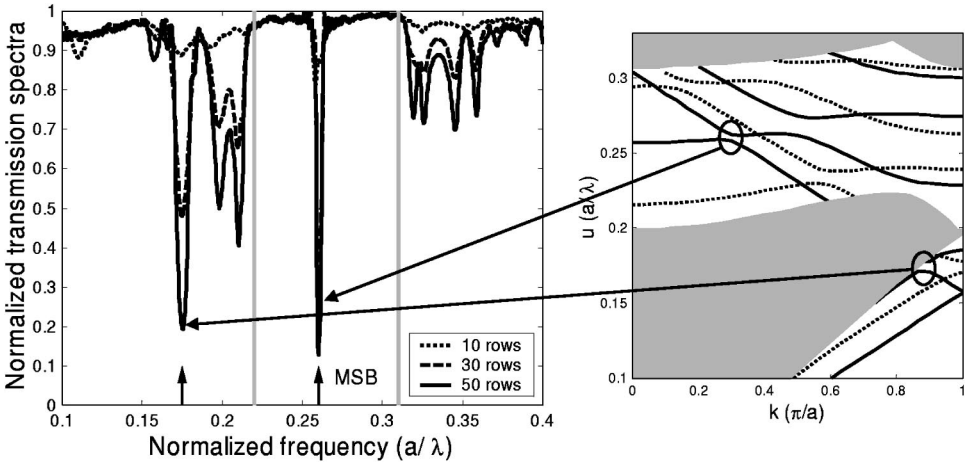

FIG. 4. The normalized transmission spectra of the fundamental mode $(m=1)$ for different lengths of the W3 waveguide.

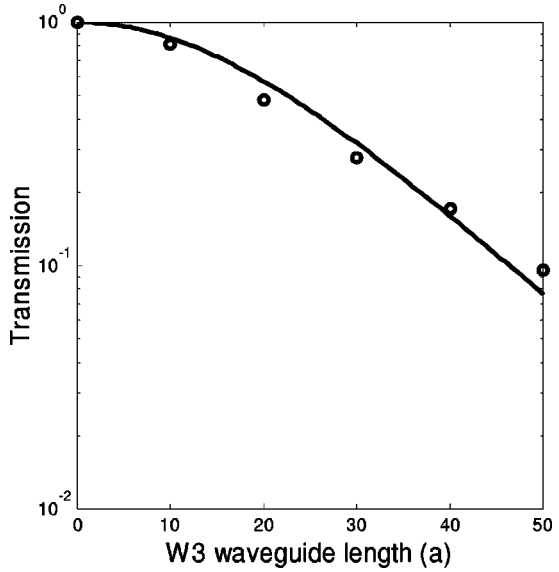

FIG. 5. The transmission as a function of the length L of the W3 PC waveguide, for the frequency inside the mini stop band 0.26 (a/λ) for the fundamental guided mode. The open circles are for calculated results, and the solid line represents $T=1-\tanh^2(\kappa L)$, where $\kappa=0.0392$ (units a^{-1}).

fundamental mode propagates into the W3 waveguide, it excites the higher order, back propagating, modes via the phase matched Bragg scattering on the periodic side walls. This results in dips in the transmission spectrum and the related mini stop bands in the modal dispersion diagram. In particular, the MSB centered at the frequency 0.26 (a/λ) results from the coupling between the $[1,-1]$ mode and the $[5,0]$ mode (see Fig. 1). From Fig. 4 one can also find another MSB centered at the frequency 0.175 (a/λ), which is out of the band gap, but below the light line. It results from the coupling between the $[1,-1]$ mode and the $[3,0]$ mode. Furthermore, it is worth to point out that other transmission dips outside the bandgap arise from the coupling between the fundamental mode and a phase matched part of the continuous spectrum of the photonic crystal modes.

For estimation of modal attenuation due to contradirectional coupling in a mini stop band, it could be of interest to extract a coupling constant. In a coupled mode language, the transmission of the waveguide is approximately given by[18]

$$T=1-\tanh^2(\kappa L)\approx 2e^{-2\kappa L}, \quad \text{for } \kappa L\gg 1, \tag{2}$$

where T is the transmission and L is the length of the waveguide. Using the data of Fig. 4 we may extract the coupling constant κ. For that purpose we position ourselves in the middle of MSB (in the band gap) 0.26 (a/λ). The transmissions at this frequency for different lengths of the W3 waveguide are shown in Fig. 5. The open circles are for calculated results, and the solid line represents $T=1-\tanh^2(\kappa L)$, with a fitted value of $\kappa=0.0392$ (in units of inverse lattice constant a^{-1}). The results follow the ''coupled mode'' results well and exhibit an approximate exponential decrease as expected for an evanescent field. The transmission drops by about -0.34 dB per lattice constant.

Finally, in order to underscore the coupling as a result between the same symmetry modes, we study the transmission properties of the second order mode $(m=2)$, which is an odd mode. Figure 6 shows the normalized transmission spectra for the mode. Similarly, the edge of the photonic band gap is indicated by gray lines. One can see from the figure that there are two mini stop bands for the second order mode. The first one, centered at the frequency 0.234 (a/λ), results from the coupling between the $[2,-1]$ mode and the $[4,0]$ mode. While the second one, centered at the frequency 0.297 (a/λ), results from the coupling between the $[2,-1]$ mode and the $[6,0]$ mode. For the frequency range from 0.24 (a/λ) to 0.29 (a/λ), there is no MSB, contrary to what was found for the fundamental mode. Therefore, albeit it may not be so easy to accomplish in practice, if one wants to avoid the MSB in this frequency range, one should excite only the second order mode in the entrance waveguide.

One thing we would like to point out is that in the presence of out-of-plane radiation losses, the position of the mode gaps should not be affected, but the spectral features in a true 3D waveguide structure, as opposed to the pure 2D structure simulated here, will be smeared out and the transmission level dropped.

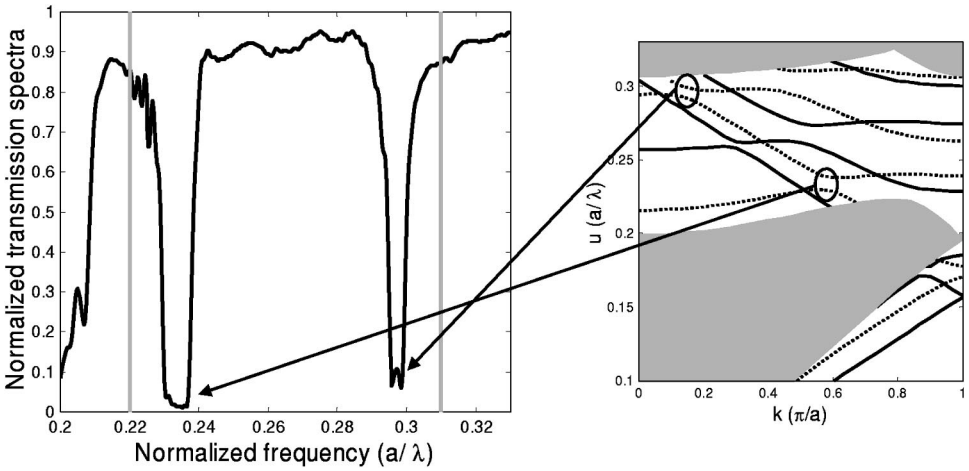

FIG. 6. The normalized transmission spectra of the second order mode $(m=2)$ for the W3 waveguide. The length of the PC waveguide is about 50 rows of air holes.

IV. CONCLUSIONS

In conclusion, we have studied the guided modes in a two-dimensional photonic crystal waveguide, which is achieved by removing three rows of air holes in a triangular photonic crystal. Using the finite-difference time-domain method, we have also studied the transmission properties through the waveguide utilizing conventional dielectric waveguides as entrance and exit waveguides. The main result of the paper is the numerical analysis of mini stop bands or (mode gaps) in the transmission spectrum. We have shown that these mini stop bands result from the coupling between the incident wave and the scattered contradirectional wave of the same inversion symmetry. Since the waveguide has a high index central region, which supports the index confinement modes, there are guided modes below the lowest photonic crystal band. Therefore the mini stop band is also observed outside the band gap. We have calculated a mode attenuation in the mini stop band in terms of a coefficient for contradirectional coupling. We also showed that a very efficient coupling between the photonic crystal waveguide and a conventional, ridge waveguides is possible.

V. ACKNOWLEDGMENTS

The authors would like to acknowledge H. Benisty, M. Rattier, S. Olivier, and C. Weisbuch for useful discussions and for friendly sharing knowledge on their experimental results on mode gaps. This work was supported by the European Commission through the IST PCIC project, and The Swedish Foundation for Strategic Research (SSF).

*Now with the Laboratory of Optics, Photonics, and Quantum Electronics, Department of Microelectronics and Information Technology, Royal Institute of Technology (KTH), Electrum 229, 164 40 Kista, Sweden.

[1] E. Yablonovitch, Phys. Rev. Lett. **58**, 2059 (1987).
[2] J. D. Joannopoulos, R. D. Mead, and J. N. Winn, *Photonic Crystals: Molding the Flow of Light* (Princeton University Press, Princeton, 1995).
[3] J. R. Wendt, G. A. Vawter, P. L. Gourley, T. M. Brennan, and B. E. Hammons, J. Vac. Sci. Technol. B **11**, 2637 (1993).
[4] T. F. Krauss, R. M. De La Rue, and S. Brand, Nature (London) **383**, 699 (1996).
[5] U. Grüning, V. Lehmann, S. Ottow, and K. Busch, Appl. Phys. Lett. **68**, 747 (1996).
[6] T. Baba, IEEE J. Sel. Top. Quantum Electron. **3**, 808 (1997).
[7] S. Y. Lin, G. Arjavalingam, and W. M. Robertson, J. Mod. Opt. **41**, 385 (1994).
[8] D. Labilloy, H. Benisty, C. Weisbuch, T. F. Krauss, R. M. De La Rue, V. Bardinal, R. Houdre, U. Oesterle, D. Cassagne, and C. Jouanin, Phys. Rev. Lett. **79**, 4147 (1997).
[9] H. Benisty, C. Weisbuch, D. Labilloy, M. Rattier, C. J. M. Smith, T. F. Krauss, R. M. De la Rue, R. Houdre, U. Oesterle, C. Jouanin, and D. Cassagne, J. Lightwave Technol. **17**, 2063 (1999).
[10] H. Benisty, D. Labilloy, C. Weisbuch, C. J. M. Smith, T. F. Krauss, D. Cassagne, A. Beraud, and C. Jouanin, Appl. Phys. Lett. **76**, 532 (2000).
[11] S. W. Leonard, H. M. van Driel, K. Busch, S. John, A. Birner, A.-P. Li, F. Müller, and U. Gösele, Appl. Phys. Lett. **75**, 3063 (1999).
[12] S. W. Leonard, H. M. van Driel, A. Birner, U. Gösele, and P. R. Villeneuve, Opt. Lett. **25**, 1550 (2000).
[13] S. G. Johnson, S. Fan, P. R. Villeneuve, J. D. Joannopoulos, and L. A. Kolodziejski, Phys. Rev. B **60**, 5751 (1999).
[14] S. G. Johnson, P. R. Villeneuve, S. Fan, and J. D. Joannopoulos, Phys. Rev. B **62**, 8212 (2000).
[15] P. Lalanne and H. Benisty, J. Appl. Phys. **89**, 1512 (2001).
[16] H. Benisty, J. Appl. Phys. **79**, 7433 (1996).
[17] H. Kogelnick and C. V. Shank, J. Appl. Phys. **43**, 2327 (1972).
[18] See, for example, T. Tamir, *Guided-Wave Optoelectronics* (Springer-Verlag, Berlin, 1988), Chaps. 2, 6.
[19] A. Mekis, S. Fan, and J. D. Joannopoulos, Phys. Rev. B **58**, 4809 (1998).
[20] K. Sakoda, T. Ueta, and K. Ohtaka, Phys. Rev. B **56**, 14 905 (1997).
[21] E. Centeno and D. Felbacq, Opt. Commun. **160**, 57 (1999).
[22] A. Taflove, *Computational Electrodynamics: The Finite-Difference Time-Domain Method* (Artech House, Norwood, 1995).
[23] K. S. Yee, IEEE Trans. Antennas Propag. **14**, 302 (1966).
[24] M. Qiu and S. He, Phys. Lett. A **266**, 425 (2000).
[25] M. Qiu and S. He, J. Appl. Phys. **87**, 8268 (2000).
[26] M. Qiu and S. He, Phys. Rev. B **61**, 12 871 (2000).
[27] J. P. Berenger, J. Comput. Phys. **114**, 185 (1994).
[28] H. Benisty (private communication).